

Supplement of Atmos. Chem. Phys., 18, 11031–11040, 2018
<https://doi.org/10.5194/acp-18-11031-2018-supplement>
© Author(s) 2018. This work is distributed under
the Creative Commons Attribution 4.0 License.



Supplement of

Revolatilisation of soil-accumulated pollutants triggered by the summer monsoon in India

Gerhard Lammel et al.

Correspondence to: Gerhard Lammel (g.lammel@mpic.de)

The copyright of individual parts of the supplement might differ from the CC BY 4.0 License.

Contents

S1 Methodology

S1.1 Chemical analysis

Table S1. QA parameters of chemical analysis

S1.2 Fugacity calculations

S1.3 Air mass history analysis

S1.4 Modelling

S1.4.1 Regional-scale 3D air pollution model

S1.4.2 1D multi-media mass balance box model

Figure S1. Schematic representation of 1D multi-media mass balance box model

S1.4.3 Model input data

Table S2. Physico-chemical properties and kinetic data of studied substances

S2 Results

S2.1 Field observations

Table S3. Observed concentrations in air

S2.2 Modelling

S2.2.1 Regional-scale 3D air pollution model

Table S4. Model predicted response of the air-soil sub-system to advection of monsoon air

Table S5. Comparison of model-predicted (3D model) and observed concentrations

S2.2.2 1D multi-media mass balance box model

Table S6. Comparison of model-predicted (1D model) and observed concentrations

Figure S2. Multidecadal 1D model predicted concentrations in the atmospheric boundary layer and diffusive air-soil exchange fluxes in the southernmost zone of India 1965-2014

Figure S3. Multidecadal 1D model predicted concentrations in the atmospheric boundary layer and topsoil various zones

S2.2.3 Model sensitivities

Table S7. Sensitivities of 1D multi-media mass balance box model output parameters to input data variation

Table S8. Comparison of 1D model-predicted under historic emissions and climate vs. under historic emissions but a fictive no-monsoon scenario

References

S1. Methodology

S1.1 Chemical analysis

The GC temperature programme for PCBs, HCHs, DDTs, PeCB and HCB was 80°C (1 min hold), then 40°C min⁻¹ to 200°C, and finally 5°C min⁻¹ to 305°C. Injection was splitless at 280°C, the injection volume was 3 µL, He was used as carrier gas at constant flow 1.5 mL min⁻¹.

The injection volume was 3 µL. PBDEs were analysed using GC-HRMS (gas chromatography with high resolution mass spectrometry) on a Restek RTX-1614 column (15 m × 0.25 mm × 0.1 µm). The resolution was set to > 10000 for BDE 28–183, and > 5000 for BDE 209. ¹³C BDEs 77 and 138 were used as injection standards. The MS was operated in EI+ mode at the resolution of >10000. The temperature programme was 80°C (1 min hold), then 20°C min⁻¹ to 250°C, followed by 1.5°C min⁻¹ to 260°C and 25°C min⁻¹ to 320°C (4.5 min hold). The injection volume was 3 µL in splitless mode at 280°C, with He used as a carrier gas at constant flow of 1 mL min⁻¹.

Recovery of native analytes ranged 88-103% for PCBs, 75-98% for OCPs, 70-95% for drin pesticides and 55-75% for PBDEs. The results for OCPs and PCBs were not recovery corrected. For PBDEs, isotope dilution method was used, the average recoveries ranged 78-128%. No replicates of sample extracts were run.

Table S1: QA parameters of chemical analysis. Instrument limits of quantification (LOQ), given as masses and concentrations, the latter for a typical sample volume (1600 m³), range of the limits of quantification (LOQs, defined as the maximum of the ILOQ and the average of field blank values plus three times their standard deviation) for soil (pg g⁻¹ or ng g⁻¹), gaseous (PUF) and filter (QFF) (pg m⁻³) of (a) OCPs, (b) PCBs and (c) PBDEs. n.t. = not targeted.

a.

	ILOQ (pg)	LOQ		
		Soil (ng g ⁻¹)	PUF (pg m ⁻³)	QFF (pg m ⁻³)
HCB	0.0062	0.01-0.03	0.38	0.0062
PeCB	0.0062	0.02-0.05	0.10	0.0062
α -HCH	0.0125	0.02-0.04	0.075	0.0125
β -HCH	0.0125	0.04-0.08	0.0125	0.0125
γ -HCH	0.0125	0.03-0.07	0.11	0.029
δ -HCH	0.0125	0.01	0.010	0.012
<i>o,p'</i> -DDE	0.0125	0.02-0.05	0.0125	0.0125
<i>p,p'</i> -DDE	0.0062	0.02-0.05	0.29	0.0062
<i>o,p'</i> -DDD	0.0062	0.03-0.06	0.0062	0.0062
<i>p,p'</i> -DDD	0.0062	0.02-0.05	0.0062	0.0062
<i>o,p'</i> -DDT	0.0125	0.03-0.05	0.037	0.0125
<i>p,p'</i> -DDT	0.0062	0.02-0.04	0.046	0.0062
Heptachlor	0.5	n.t.	0.027	0.5
Aldrin	0.5	n.t.	0.054	0.5
Dieldrin	0.5	n.t.	0.13	0.5
Endrin	0.5	n.t.	0.43	0.5
α -chlordane	0.5	n.t.	0.026	0.5
γ -chlordane	0.5	n.t.	0.024	0.5

α -endosulfan	0.5	n.t.	0.077	0.5
β -endosulfan	0.5	n.t.	0.13	0.5
Endosulfan sulfate	0.5	n.t.	0.31	0.5
Mirex	0.5	n.t.	0.012	0.5

b.

	ILOQ (pg)	LOQ		
		Soil (ng g ⁻¹)	PUF (pg m ⁻³)	QFF (pg m ⁻³)
PCB28	0.0062	0.01-0.03	0.39	0.0062
PCB52	0.0062	0.02-0.03	0.058	0.0062
PCB101	0.0062	0.04-0.08	0.036	0.0062
PCB118	0.0062	0.02-0.03	0.0062	0.0062
PCB153	0.0062	0.03-0.05	0.051	0.0062
PCB138	0.0125	0.03-0.05	0.034	0.0125
PCB180	0.0062	0.02-0.05	0.024	0.0062

c.

	ILOQ (pg)	LOQ		
		Soil (pg g ⁻¹)	PUF (pg m ⁻³)	QFF (pg m ⁻³)
BDE28	1.45	0.29-0.35	0.0016	0.0018
BDE47	0.27	0.054	0.0043	0.0013
BDE100	0.48	0.096-0.81	0.00051	0.00065
BDE99	0.81	0.162	0.00081	0.0011
BDE154	2.80	0.25-0.31	0.0029	0.0036
BDE153	5.19	0.40-0.68	0.0054	0.0052
BDE183	2.55	0.48-0.88	0.0028	0.0026

S1.2 Fugacity calculations

Fugacities of OCPs in soil (f_s) and air (f_a) were calculated as (Harner et al., 2001):

$$(S1) \quad f_s = c_s H(T) / (0.411 \phi_{OM} K_{OW})$$

$$(S2) \quad f_a = c_a R_g T$$

with c_s , c_a being the concentrations in the media (mol m^{-3}), $H(T)$ is the temperature dependent Henry's law constant ($\text{Pa m}^3 \text{mol}^{-1}$), ϕ_{OM} is the mass fraction of organic matter in soil, K_{OW} is the octanol–water partitioning coefficient, R_g is the universal gas constant ($8.314 \text{ J mol}^{-1} \text{ K}^{-1}$), and T is temperature (K). The factor 0.411 improves the correlation between the soil-air partitioning coefficient and K_{OW} (Hippelein and McLachlan, 1998; Meijer et al., 2003a). $H(T)$ was obtained using the van't Hoff equation:

$$(S3) \quad \ln(H_1/H_2) = -\Delta H_{\text{vap}}(1/T_1 - 1/T_2)/R_g$$

with temperatures T_1 and T_2 (K), H_1 and H_2 being the Henry's law constants at these temperatures, and enthalpy of vaporisation ΔH_{vap} (J mol^{-1}).

Physico-chemical data were taken from literature (Li et al., 2003; Xiao et al., 2004; Shen and Wania, 2005). 48h-means of the soil temperature are input into equ. (S1), assumed to be given by the 48h-mean near-ground air temperature. Soil density, ρ_s , needed to calculate c_s (mol m^{-3}) from measured values (in ng g^{-1}), is unknown and assumed to be equal to the mean value for this region, 1.04 g cm^{-3} (taken from the global model, MCTM, see S1.4.2). It is assumed that particulate organic matter (OM) mass equals 1.67 times the total organic carbon mass, TOC.

Contributions to the uncertainty of the fugacity ratio, f_s / f_a , are the uncertainties of measured concentrations c_s ($\pm 20\%$), c_a ($\pm 20\%$), Henry coefficient and OM/TOC. Values $0.3 < f_s / f_a < 3.0$ are conservatively considered to not safely differ from phase equilibrium (as commonly accepted e.g., Bruhn et al., 2003; Castro-Jiménez et al., 2012; Zhong et al., 2012; Mulder et al., 2014).

S1.3 Air mass history analysis

The discrepancies of dating of the onset of monsoon, based on hydrological, convection or circulation indices (Wang and Fan, 1999; Wang et al., 2001; Fasullo and Webster, 2003), or on local weather monitoring (IMD, 2014) are about ± 1 day. In 2014, monsoon arrival in Kerala was dated to 6 June (IMD, 2014; Devi and Yadav, 2015). As the origin of air masses arriving in southern India switch from northern hemispheric to southern hemispheric with the onset of southwest monsoon, the tracking of air mass histories allows for higher temporal resolution. We analysed air masses histories, 3-hourly, using the HYSPLIT model (Draxler and Rolph, 2003) and the FLEXPART Lagrangian dispersion model (Stohl et al., 1998, 2005) at various arrival heights, 0-6000 m a.s.l.. The meteorological data ($0.5^\circ \times 0.5^\circ$ resolution, 3-hourly) were taken from ECMWF for FLEXPART runs and from NCEP for HYSPLIT runs. For FLEXPART runs, Lagrangian particles were released continuously.

S1.4 Modelling

S1.4.1 Regional-scale 3D air pollution model

Model: WRF-Chem integrates meteorological, gas-phase chemistry, and aerosol components. The planetary boundary layer parameterisation uses the Mellor–Yamada–Janjic scheme (Janjic, 1994) and Smagorinsky first-order closure for vertical and horizontal sub-grid-scale fluxes, respectively. Surface layer and soil-atmosphere interaction parameterisations follow Janjic, 1994, and Chen and Dudhia, 2001, respectively. Cumulus is parameterised using the Grell-3D Ensemble scheme (Grell and Devenyi, 2002). Hydrometeors (cloud water and ice, rain, snow and graupel) microphysics follows the Purdue–Lin scheme (Lin et al., 1983). Short- and longwave radiation are calculated following the Goddard scheme (Chou and Suarez, 1994) and Mlawer et al., 1997, respectively. Photolysis rates are derived on an hourly basis using the Fast-J scheme (Wild et al., 2000). A modal aerosol is described based on the Modal Aerosol Dynamics Model for Europe (MADE; Ackermann et al., 1998). Secondary organic aerosol is diagnosed using the Secondary Organic Aerosol Model (SORGAM; Schell et al., 2001). Modes considered by MADE/SORGAM are the nucleation, accumulation and coarse modes. The model has recently been extended by parameterisations for air-soil exchange and gas-particle partitioning (Mu et al.,

2017) such as to describe the cycling of semivolatile organics of organic substances. Gas-particle partitioning is described using a single-parameter linear free-energy relationship, an absorption model (K_{oa} model; Finizio et al., 1997).

The air-soil gas exchange flux is described by a parameterisation of the Jury model (e.g. Hansen et al., 2004; Jury et al., 2003).

$$(S4) \quad F_c = -v_s [(1-\theta) c_a - c_s/K_{sa}]$$

where v_s is the exchange velocity between the air and the soil ($m\ s^{-1}$), θ is the particulate mass fraction, c_a and c_s are the air and soil concentrations ($kg\ m^{-3}$), respectively and K_{sa} is the soil-air exchange partitioning coefficient (dimensionless). Therefore, a positive F_c indicates volatilisation while a negative value characterizes deposition. The exchange velocity between the air and the soil, v_s , is defined as (Strand and Hov, 1996; Hansen et al., 2004):

$$(S5) \quad v_s = [D_G^{air} f_a^{10/3} + D_L^{water} I^{10/3} K_{aw}(T)^{-1}] (1 - f_l - f_a)^{-2} / (h_s/2)$$

where D_G^{air} and D_L^{water} are the diffusion coefficient in air and water ($m^2\ s^{-1}$), respectively, f_a and f_l represent the air and liquid fraction in soil (dimensionless) and K_{aw} is the air-water partitioning coefficient (dimensionless). The influence of temperature on K_{aw} was taken into account using van't Hoff equations. K_{sa} used in this study were defined as (Karickhoff, 1981):

$$(S6) \quad K_{sa} = 0.411 f_{OC} \rho_s K_{OA}(T)$$

where f_{OC} is the fraction of organic carbon in soil ($0.010\ g_{OC}\ g_{soil}^{-1}$; upper value in the range of values spanned across the climate zones of India, see below S1.4.2), ρ_s is the soil density ($1.35\ kg\ L^{-1}$; estimate, Jury et al., 2003), K_{OA} is the temperature dependent octanol-air partitioning coefficient and 0.411 is a constant with units of $L\ kg^{-1}$. In agreement with the experimental soil sampling, the model soil is a 0.05 m thick layer which was assumed to contain 50% of soil, 30% of water and 20% of air (Jury et al; 2003).

Substances:

For modelling each 2 PCBs and HCH isomers are selected. These 4 POPs span a wide range of physico-chemical properties i.e., from low to moderate volatile and from lipophilic to moderately water soluble (Table S4). DDT could not be included as its emissions are insufficiently known

for an episode simulation: The emission time (often twice i.e., once during summer and once during monsoon; NVBDCP, 2009) and emission factor (to account for release of indoor sprayed DDT to the ambient air) are basically unknown. Similarly, PeCB, HCB and PBDEs could not be covered by modelling, because of lack of emission estimates.

Emissions: Primary emissions are considered for PCBs (gridded data, upper emission estimate for the year 2014; Breivik et al., 2007) and distributed across grid cells for India. During the episode PCB emissions are temperature driven, scaled according to vapour pressure. Herewith, it is accounted for the fact that the prevailing sources i.e., buildings and open installations, are following ambient temperature variation (as found elsewhere in post-ban times; Gasic et al., 2010). Suspected on-going emissions of α - and γ -HCH, partly legal, but not reported (Sharma et al., 2014), are neglected.

Boundary conditions: In the model experiment, air concentrations representing pre-monsoon or monsoon background conditions are input continuously at all boundaries of the domain. For monsoon conditions, the background air concentrations, advected to the continent from the model domain boundaries are appropriately represented by the concentrations measured on site after onset of the monsoon (mean of the period 6-10 June 2014), while for pre-monsoon conditions they are represented by the concentrations measured on site before mixing with monsoon air (we adopt the mean of the period 30 May – 2 June 2014). PCB and HCH air concentrations measured on site are appropriate, as these are representing background conditions. Adopting these measured values, we implicitly assume that concentration changes along transport from the domain boundaries over sea to land will be negligible, and trust that propagation of southwest monsoon northward is well captured by model (nudged) meteorology. Hereby, in order to mimick the northward propagation of monsoon in the model experiment, the boundary conditions are switched from pre-monsoon to monsoon conditions progressively from south to north by $0.75^{\circ}\text{N}/\text{day}$, passing 10°N (latitude of Munnar) on 6 June. The vertical profiles and the tendencies of the atmospheric concentrations of the pollutant species at the boundaries are scaled (or adopted) according to the vertical profile and the concentration at the site, respectively, of a long-lived tracer, namely CO of the global chemistry model output used for boundary conditions in WRF-Chem i.e., MOZART (Emmons et al., 2010). In the control

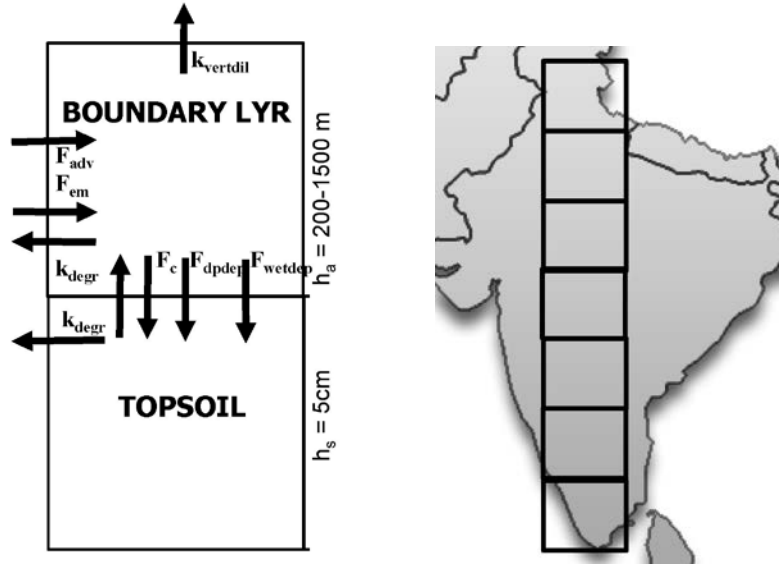
experiment, a second run, the pre-monsoon background conditions are input throughout the whole run.

S1.4.2 1D multi-media mass balance box model

Compartments simulated

Although small mass fractions of lipophilic substances ($\log K_{oa} \geq 6$) cycling in continents are stored in above- and below-ground parts of vegetation (Calamari et al., 1991; Meijer et al., 2003b; Lammel et al., 2007) and in freshwater and ice, we refrain from including vegetation, freshwater or cryosphere compartments, apart from air and soil (Fig. 1). Freshwater/wetlands and glaciers are neglected, because of the small area they cover on the Indian subcontinent, and largely peripheral locations. As to vegetation, bioaccumulation of lipophilic substances in leaves and needles follows equilibrium with air and soil typically within 2 months for the most hydrophobic chemicals, shorter for less hydrophobic (Paterson and Mackay, 1991; Paterson et al., 1994). Dry particle and wet deposition fluxes, F_{dpdep} and F_{wetdep} , are parameterized such as to include various relevant canopies and account for enhanced air-surface transfer by high canopies (McLachlan and Horstmann 1998). Pollutants' clearance rates of the studied substances from vegetation are not available, therefore, in lack of better knowledge degradation within vegetation is commonly assumed to follow the same kinetics as in the soil, k_{degr} . Hence, while vegetation cycling of pollutants mediates air-surface exchange on seasonal and shorter time scales (e.g., Bao et al., 2016), it is considered to not significantly bias the chemodynamics on the multi-year time scale (Scheringer and Wania, 2003). Moreover, in tropical climate, air-surface exchange is not expected to be influenced by seasonally changing vegetation compartment volume, unlike in temperate climate (Wania and McLachlan 2001). In summary, short-term fluctuations of model predicted air-surface exchange flux, F_c , may be biased by the neglect of explicit air-vegetation and soil-vegetation gas exchanges and are not studied here.

Fig. S1. Schematic representation of 1D multi-media mass balance box model: Processes in the atmospheric boundary layer and topsoil including air-surface exchange (F_c), emission (F_{em}), advection (F_{adv}), dry particle deposition (F_{dpdep}), wet deposition (F_{wetdep}), removal from the residual layer ($F_{vertdil}$), and degradation (k_{degr}). Series of 7 two-boxes with heights h_a and h_s , connected by F_{adv} , spanning in total 7.4-33.4°N.



Mass balance equations:

$$(S7) \quad \frac{dba}{dt} = - [(1-\theta) k_{OH}^{(2)} c_{OH} + v_{dep} \theta / h_{mix} + W_t] \times b_a + F_c + F_{em}$$

$$(S8) \quad \frac{dbs}{dt} = + (v_{pdep} \theta / h_{mix} + W_t) \times b_a - F_c - k_s^{(1)} b_s$$

where b_a and b_s are the air and soil burden (kg m^{-2}), respectively, θ is the particulate fraction (dimensionless), $k_{OH}^{(2)}$ is the 2nd order degradation rate coefficient of the reaction with OH radicals ($\text{cm}^3 \text{ molec}^{-1} \text{ s}^{-1}$), c_{OH} is the OH concentration in the air (molec cm^{-3}), v_{pdep} is the dry particulate deposition velocity (m s^{-1}), h_{mix} is the boundary layer (BL) depth (m), W_t is the scavenging coefficient (s^{-1}), F_c is the air-surface exchange flux ($\text{kg m}^{-2} \text{ s}^{-1}$), F_{em} is the emission flux ($\text{kg m}^{-2} \text{ s}^{-1}$), $k_s^{(1)}(T)$ is the 1st order degradation rate in the soil (s^{-1} ; default temperature dependence assuming doubling per 10 K increase). The particle deposition velocity $v_{dep p}$ was derived using an empiric relationship for particle size dependent lifetime (Jaenicke, 1988):

$$(S9) \quad v_{dep p}(D) = h_{mix} / \tau_{dry}(D) = h_{mix} \times [(D/0.6)^2 + (D/0.6)^{-2}] / b$$

where b is a constant and D is the mean particle size (μm). We adopted $b = 10^6 \text{ s}$, as this leads to $v_{\text{dep},p} > 0.01 \text{ cm s}^{-1}$ for $h_{\text{mix}} = 200\text{-}8000 \text{ m}$ as suggested by field studies covering a wide range of canopies (Ruijgrok et al., 1995; Pryor et al., 2008) and $D = 0.2 \mu\text{m}$ for all SOCs investigated in agreement with previous field studies (Landlová et al., 2014; Degrendele et al., 2016; Zhu et al., 2017). The wet scavenging coefficient, W_t , is derived as the ratio of the wet deposition flux, F_{wet} , and the air burden, b_a , both adopted from global multicompartment chemistry-transport model (MCTM) output for the study area (Semeena et al., 2006; Lammel and Stemmler, 2012). In the MCTM, the air burden, b_a , is fed from advection and primary and secondary emissions, the latter include also vegetation surfaces, apart from soils and other ground surfaces. Therefore, W_t is implicitly accounting for vegetation canopies.

The air-surface gaseous exchange flux, F_c , is defined as above (see S1.4.1). Again, K_{sa} is calculated using fraction of organic carbon in soil, f_{OC} , and soil density, ρ_s (Karickhoff, 1981; see above S1.4.1). f_{OC} , and ρ_s in the 7 zones are adopted from MCTM input i.e., globally mapped soil data (Batjes, 1996; Dunne and Willmott, 1996; Semeena et al., 2006), and range $0.0033\text{-}0.0104 \text{ g}_{\text{OC}} \text{ g}_{\text{soil}}^{-1}$ and $1.04\text{-}1.45 \text{ kg L}^{-1}$, respectively.

Air and soil concentrations were calculated from the air and soil burden as $c_a = b_a/h_{\text{mix}}$ and $c_s = b_s/h_s$ with h_s the soil depth (m). In agreement with the experimental soil sampling, the model soil depth is 0.05 m. Monthly mean concentrations of the hydroxyl radical, c_{OH} , are extrapolated from a climatology (Spivakovsky et al., 2000; 3-monthly data) and range $(0.38\text{-}2.09) \times 10^6 \text{ molec cm}^{-3}$ across the 7 zones and all months. Neighboring cells are connected by southward advection, replacing c_a exactly once per time step (F_{adv} , $\Delta t = 7 \text{ h}$). Substance specific input parameters, including their temperature dependencies, are listed in Table S2. The dry particulate deposition flux was defined as:

$$(S10) \quad F_{\text{drydep}} = v_{\text{dep}} \theta c_a$$

θ is calculated using gas-particle partitioning models, namely an absorption model (K_{oa} ; Finizio et al., 1997) for chlorinated substances. Total particulate matter and OM concentrations in near-ground air are taken from a global chemistry-climate model (ECHAM/MESSy Atmospheric Chemistry) with a modal aerosol sub-model (HAM; Pringle et al., 2010).

Advection and boundary layer depth: India is represented as 7 zones in N-S direction, each 3.75°N wide (7.4-33.4°N; Fig. S1). The prevailing wind direction throughout most of the year and across most of the zones is westerly, with a northerly component, actually not linked to a particular monsoon phase. The annual mean northerly component at 850 hPa (≈ 1400 m a.s.l.) across the 7 zones amounts to 1.63 m s^{-1} (in the longitude band 76.85-80.65°E), which corresponds to a characteristic advection time of 7 h between neighbouring latitudinal zones. 850 hPa is chosen to represent the altitude of prevailing transport within the BL. BL depth, h_{mix} , varies in the range 550-1300 m during monsoon and somewhat higher, 750-1900 m in the pre-monsoon season (1965-2001 monthly means for the 7 zones in 7.4-33.4°N/76.85-80.65°E taken from ERA-40 re-analysis data; ECMWF, see also Patil et al., 2013). The terrain height varies across the 7 zones between ≈ 100 m in the coastal plain of Tamil Nadu and the Indo-Gangetic Plain, and > 1000 m in the central highland and Himalayan foothills. The diurnal variation of the boundary layer depth (at 12:00 and 18:00h UTC, ERA-40 data, ECMWF) is considered to derive a pollutant loss term from the BL into the free troposphere: before sunrise, 10% of the pollutant burden which resides in the residual layer (e.g., Stull, 1988) is removed, such that only 90% is preserved for being included into the BL following the morning increase of BL depth (corresponding to a vertical dilution with a varying rate coefficient k_{vertdil}).

Substances: For modelling, 2 PCBs, one HCH isomer (α -HCH) and DDT were selected. These 4 POPs span a wide range of physic-chemical properties i.e., from very low to moderate volatility and from lipophilic to moderately water soluble (Table S4). On the multidecadal time scale, DDT is covered too, despite the limitations related to emissions since the ban in agriculture, 1989 (see S1.4.1, above).

Emissions: Historical, gridded primary emission data were adopted for the 7 latitudinal zones. Such gridded data were available for α -HCH (annual data; Li et al., 2000), DDT (extrapolated from every tenth year; Semeena and Lammel, 2003), and PCBs (annual data; Breivik et al., 2007; upper estimates used). For post-ban remaining emissions 10^{-5} of the last pre-ban emissions are assumed for α -HCH. For DDT applied indoors in governmental health programs of India (since 1990), total amounts emitted were available (extrapolated from every tenth year; Pacyna et al., 2010). It is assumed that the DDT emissions of 1980 had continued until the ban, 1989. DDT usage in India after 1989 is inconsistently reported (e.g., 1126 or 3347 t in 2010; Pacyna et al.,

2010; UNEP, 2016). The lower values were adopted. For PCBs and pesticides used in agriculture (α -HCH, DDT) annual sums were homogeneously entered throughout the year. However, post-ban PCB emissions are mostly from buildings and open installations and, therefore, are simulated to be driven by vapour pressure (scaled to mean hourly ambient temperature variation at a central India site, 22°N). Furthermore, as DDT application since the year 1990 have been mostly twice per year, before and during SW monsoon, with some local flexibility (NVBDCP, 2009), temporally homogeneous application to all land is assumed in the model throughout January to August, while zero emissions are assumed throughout September to December.

Initialisation of simulation: The initial soil concentrations of all compounds investigated were set to zero at t_0 (1965). Initial air concentration is considered for the northernmost cell, while the other cells receive advection from the northern neighbor cell. Advection into the BL box of the northernmost zone is from the northern hemispheric background during non-monsoon months and zero during monsoon months. For non-monsoon months, annual mean levels observed at the Himalayas foothills (site Surkanda Devi, 2200 m a.s.l., 2006-07; Pozo et al., 2011) are considered for PCBs, for other years scaled with the emissions.

Time dependent input parameters: emission flux (annual), (monthly and day/night), mixing height (monthly, daily 10% loss into residual layer), air temperature (monthly, for gas-particle partitioning), soil temperature (monthly, for air-surface exchange flux), wet deposition flux (monthly).

Model evaluation and sensitivity study: Regarding the input data uncertainties, concentrations in air and soil are predicted well, except for DDT which concentrations in air, c_a , are largely overestimated (Table 6b). This results probably from the very uncertain emission estimates for recent years (above, S1.4.1). Furthermore, as part of the substance is sorbed to aerosol particles (particulate mass fraction $\theta > 0$; Landlová et al., 2014, the mean value observed at the site was $\theta = 0.04$), lifetime in air is strongly influenced by wash-out of particles and might be affected by discrepancies between predicted and observed precipitation. DDT concentration in soil, c_s , is overestimated, too, and very sensitive to k_{soil} , which is an estimate only (no experimental data available). For PCB28 the soil concentration is underpredicted by one order of magnitude.

The direction of diffusive air-surface exchange flux, F_c , in southern India is well predicted for all substances. The effect of onset of SW monsoon on the magnitude of the air-surface exchange flux is well predicted for the pesticides studied, but out of phase for the PCBs. The observed seasonality of F_c (Fig. S4) results from the combination of emission and deposition patterns. In the model, PCB sources, both primary and secondary emissions are following ambient temperature (primary emissions i.e., evaporation from buildings, facilities, scaled with vapour pressure). Maximum seasonal concentrations of DDT compounds in the outflows from the Indo-Gangetic Plain into the Himalayas had been observed during June-July, which was explained by flooding-related application (Sheng et al., 2013).

In general, long-term budgeting of POPs cycling is limited by data availability, with degradation rates in soil being estimated from a wide range of observed disappearance rates. Declining DDT and HCH levels in soil, modelled in this study, were based on upper estimates of degradation rates (Mackay et al., 2006), and may be uncertain by one order of magnitude on this spatial scale. Apart from DDT and HCH, also the concentration and, hence, air-surface exchange flux of PCB28 is sensitive to k_{soil} . The sensitivities of 1D multi-media mass balance box model output parameters to input data variation is listed in Table S7.

S1.4.3 Model input data

Table S2. Physico-chemical properties and kinetic data of studied substances

Property	PCB28	PCB153	α -HCH	γ HCH	<i>p,p'</i> -DDT
Saturation vapour pressure (p_{sat}) (mPa)	13.06 ^(b,d)	0.101 ^(b,d)	3.3 ^(m)	76 ^(m)	0.025 ^(a,c)
Henry's Law coefficient (Pa m ³ mol ⁻¹)	30.4 ^(d)	19.4 ^(d)	0.73 ^(m)	0.30 ^(m)	1.1 ^(h)
Water solubility at 298 K (mg L ⁻¹)	0.23 ^(d)	1.11 \times 10 ^{-3(d)}	2.0 ^(m)	7.3 ^(m)	0.149 ^(d)
Enthalpy of vapourisation (ΔH_{vap}) (kJ mol ⁻¹)	89.3 ^(g)	103.5 ^(f)	67.0 ^(m)	74.8 ^(m)	118 ^(e)
Enthalpy of solution (ΔH_{sol}) (kJ mol ⁻¹)	27 ^(e)	27 ^(e)	7.63 ^(m)	15.1 ^(m)	27 ^(e)
Octanol-air partitioning coefficient (log K_{oa}) at 298 K	8.06 ⁽ⁱ⁾	9.44 ⁽ⁱ⁾	7.47 ^(m)	7.75 ^(m)	9.73 ^(h)
OH gas-phase rate coefficient ($k_{\text{OH-g}}$) at 298 K (10 ⁻¹² cm ³ moles ⁻¹ s ⁻¹)	1.06 ^(j)	0.164 ^(j)	0.15 ⁽ⁿ⁾	0.19 ⁽ⁿ⁾	0.5 ^(e)
$\Delta E/R$ of OH reaction (K ⁻¹)	0 ^(e)	0 ^(e)	-1300 ⁽ⁿ⁾	-1710 ⁽ⁿ⁾	0 ^(e)
Degradation rate coefficient in soil (k_{soil}) (10 ⁻⁹ s ⁻¹)	19.3 ^(k,l)	0.35 ^(k,l)	110 ^(o,l)	20 ^(c,l)	4.05 ^(o,l)

^(a) at 293K

^(b) at 298K

^(c) Hornsby et al., 1996

^(d) Li et al., 2003

^(e) estimated

^(f) Puri et al., 2001

^(g) Puri et al., 2002

^(h) Shen and Wania, 2005

⁽ⁱ⁾ $K_{\text{oa}} = K_{\text{ow}}/K_{\text{aw}}$; K_{ow} from Li et al., 2003, K_{aw} based on water solubility and vapour pressure

^(j) Anderson and Hites, 1996

^(k) Wania and Daly, 2002

^(l) assumed to double per 10 K temperature increase (EU, 1006)

^(m) Xiao et al., 2004

⁽ⁿ⁾ Brubaker and Hites, 1998

^(o) Beyer et al., 2000

S2 Results

S2.1 Field observations

Table S3. Observed concentrations in air, c_a (sum of gaseous and particulate phases) of (a) pesticides, (b) PCBs, (c) PBDEs (pg m^{-3}) and (d) organic and elemental carbon ($\mu\text{g m}^{-3}$) during the entire campaign (5 May - 10 June) and 96 h periods shortly before (30 May-2 June) and after (6-10 June) onset of southwest monsoon.

a.

	Mean (entire campaign 5 May - 10 June 2014)	Pre-monsoon period 30 May - 2 June 2014	Monsoon period 6-10 June 2014
HCB	8.01	11.2	8.25
PeCB	0.72	1.16	0.13
α -HCH	4.70	6.37	1.34
β -HCH	0.66	0.72	0.19
γ -HCH	4.15	4.14	0.88
δ -HCH	0.77	0.60	0.33
ε -HCH	0.11	0.10	0.01
<i>o,p'</i> -DDE	0.53	0.58	0.17
<i>p,p'</i> -DDE	2.23	1.87	0.35
<i>o,p'</i> -DDD	0.23	0.35	0.11
<i>p,p'</i> -DDD	0.30	0.39	0.06
<i>o,p'</i> -DDT	1.84	2.36	0.62
<i>p,p'</i> -DDT	1.33	1.38	0.43
Heptachlor	0.004	<0.058	<0.026
Aldrin	0.016	<0.12	<0.052
Dieldrin	0.11	0.032	0.049
Endrin	0.39	<0.92	<0.41
α -chlordan	0.035	0.041	0.009
γ -chlordan	0.055	0.050	<0.024
α -endosulfan	2.72	3.53	0.80
β -endosulfan	0.26	0.20	<0.13
endosulfan sulfate	1.76	2.61	0.41
Mirex	0.021	0.012	0.013

b.

	Mean	Pre-monsoon period 30 May – 2 June 2014	Monsoon period 6-10 June 2014
PCB28	10.8	10.1	5.51
PCB52	4.54	4.41	2.36
PCB101	0.78	0.64	0.34
PCB118	0.46	0.32	0.18
PCB153	0.58	0.40	0.21
PCB138	0.43	0.28	0.14
PCB180	0.38	0.13	0.13

c.

	Mean	Pre-monsoon period 30 May – 2 June 2014	Monsoon period 6-10 June 2014
BDE28	0.013	0.002	0.025
BDE47	0.031	0.008	0.025
BDE100	0.005	<0.002	0.007
BDE99	0.018	0.003	0.022
BDE154	0.006	<0.009	0.002
BDE153	0.008	<0.017	<0.003
BDE183	0.028	0.004	<0.003

d.

	Mean	Pre-monsoon period 30 May – 2 June 2014	Monsoon period 6-10 June 2014
Organic carbon	4.28	3.19	0.86
Elemental carbon	1.09	0.80	0.08

S2.2 Modelling

S2.2.1 Regional-scale 3D air pollution model

Table S4. 3D model predicted response of the air-soil sub-system to advection of monsoon air at selected sites in southern, central and northern India, (a) concentrations in air under monsoon, c_{pred} (pg m^{-3}) and change upon onset, $\Delta c_{\text{pred}}/c_{\text{pred}}$ (%) ^a in brackets and (b) change of diffusive air-soil gas exchange flux upon onset of monsoon, ΔF_c ($\text{pg m}^{-2} \text{h}^{-1}$, positive upward) and $\Delta F_{\text{pred}}/F_{\text{pred}}$ (%) ^b in brackets. Monsoon/pre-monsoon periods are 8-10 June/1-3 June, 20-22 June/8-10 June, and 28-30 June/20-22 June at 9, 22 and 29°N, respectively.

a.

c	S India (Munnar, 9°N)	C India (22°N)	N India (29°N)
α -HCH	1.1 (-79%)	2.2 (-17%)	4.7 (-4%)
γ -HCH	0.73 (-83%)	1.7(-19%)	3.9 (-4%)
PCB28	1.2 (-79%)	2.4 (-17%)	5.2 (-4%)
PCB153	0.37 (-40%)	0.34 (-11%)	0.46 (+1%)

b.

F	S India (Munnar, 9°N)	C India (22°N)	N India (29°N)
α -HCH	0.29 (+ 5%)	0.09 (+ 1%)	0.004 ($\pm 0\%$)
γ -HCH	0.78 (+ 3%)	0.19 ($\pm 0\%$)	0.007 ($\pm 0\%$)
PCB28	0.11 (+ 4%)	0.04 (+ 8%)	0.002 ($\pm 0\%$)
PCB153	0.02 (+11%)	0.002 (+97%)	<0.0001 (+1%)

^a defined as $(\Delta c_{\text{exp}} - \Delta c_{\text{ctrl}})/c_{\text{premonsoon}}$, with: $\Delta c = c_{\text{monsoon}} - c_{\text{premonsoon}}$

^b defined as $(\Delta F_{\text{exp}} - \Delta F_{\text{ctrl}})/F_{\text{premonsoon}}$, with: $\Delta F = F_{\text{monsoon}} - F_{\text{premonsoon}}$

Table S5. Comparison of model-predicted (3D model) and observed air concentration change with observations, concentrations under monsoon, c_{obs} , c_{pred} (pg m^{-3}) and change $\Delta c/c(\%)$ ^a upon onset, $\Delta c = c_{\text{monsoon}} - c_{\text{premonsoon}}$ (3D model, for Munnar, 9°N)

	c_{obs} ($\Delta c_{\text{obs}}/c_{\text{obs}}$)	c_{pred} ($\Delta c_{\text{pred}}/c_{\text{pred}}$)
α -HCH	1.3 (-83%)	1.1 (-79%)
γ -HCH	0.88 (-87%)	0.73 (-83%)
PCB28	5.5 (-55%)	1.2 (-79%)
PCB153	0.21 (-55%)	0.37 (-40%)

S2.2.2 1D multi-media mass balance box model

Table S6. Comparison of model-predicted and observed (a) air concentration change with observations, concentrations under monsoon, c_{obs} , c_{pred} (pg m^{-3}) and change $\Delta c/c(\%)$ ^a upon onset, $\Delta c = c_{\text{monsoon}} - c_{\text{premonsoon}}$ (3D model, for Munnar, 9°N), (b) in air (pg m^{-3}) and soil (pg g^{-1}) (1D model for southern zone; pre-monsoon = May average, monsoon = June average), and (c) historically. N = North India, S = South India

a.

	c_{obs} ($\Delta c_{\text{obs}}/c_{\text{obs}}$)	c_{pred} ($\Delta c_{\text{pred}}/c_{\text{pred}}$)
α -HCH	1.3 (-83%)	1.1 (-79%)
γ -HCH	0.88 (-87%)	0.73 (-83%)
PCB28	5.5 (-55%)	1.2 (-79%)
PCB153	0.21 (-55%)	0.37 (-40%)

b.

	Air				Soil	
	Pre-monsoon		Monsoon		Pre-monsoon	
	Observed	Modelled	Observed	Modelled	Observed ^b	Modelled
α -HCH	7.73	11	1.13	1.4	0.010-0.036	0.0011
<i>p,p'</i> -DDT	1.54	70	0.33	75	0.060	0.061
PCB28	10.54	3.3	4.89	0.74	0.054-0.060	0.0013
PCB153	0.47	0.43	0.18	0.38	0.034-0.040	0.023

c.

		Air		Soil	
		Predicted	Observed	Predicted	Observed
α -HCH	1965-74	N 10^3 - 10^5 S 2×10^3 - 2×10^5		1-20	
	1975-84	N 10^4 - 2×10^5 S 2×10^4 - 2×10^5		2-40	
	1985-94	N 0.1- 2×10^5 S 0.03- 3×10^5	S 1.5-35.5 ^{cc}	N 0.02-40 S 0.001-40	N 17-46 ^h S 70-90 (<5- \approx 400) ^j
	1995-2004	N 6-20 S 3-20		N 0.02-0.04 S 0.001-0.003	N 1.6-835 ^{ci}
	2005-14	N 6-20 S 3-20	NS 50-670 ^{cg} S 100-360 ^{cf}	N 0.02-0.04 S 0.001-0.003	
DDT	1965-74	N 10^3 - 2×10^4 S 4×10^2 - 2×10^4		N 0.6-5 S 1-20	
	1975-84	N 2×10^3 - 5×10^4 S 8×10^3 - 5×10^4	S 0.16-5.93 ^{de}	N 5-20 S 20-30	
	1985-94	N 150- 5×10^4 S 8×10^3 - 5×10^4		N 2-20 S 2-30	N <1-45 ^h \approx 0.6 (<0.1- \approx 2) ^j
	1995-2004	N 20-2000 S 2-7000	NS 20-1010 ^{dg} S 120-140 ^{df}	N 0.3-6 S 0.2-6	N 14-934 ^{dh}
	2005-14	N 10-200 S 0.8-400		N 0.02-1 S 0.02-0.4	

^a for predicted defined as $(\Delta c_{\text{exp}} - \Delta c_{\text{ctrl}})/c_{\text{premonsoon}}$, with: $\Delta c = c_{\text{monsoon}} - c_{\text{premonsoon}}$

^b range of 3 soil samples, except for DDT (forest soil sample only)

^c Σ_4 HCH

^d DDX

^e coastal town (Rajendran et al., 1999)

^f rural (Pozo et al., 2011)

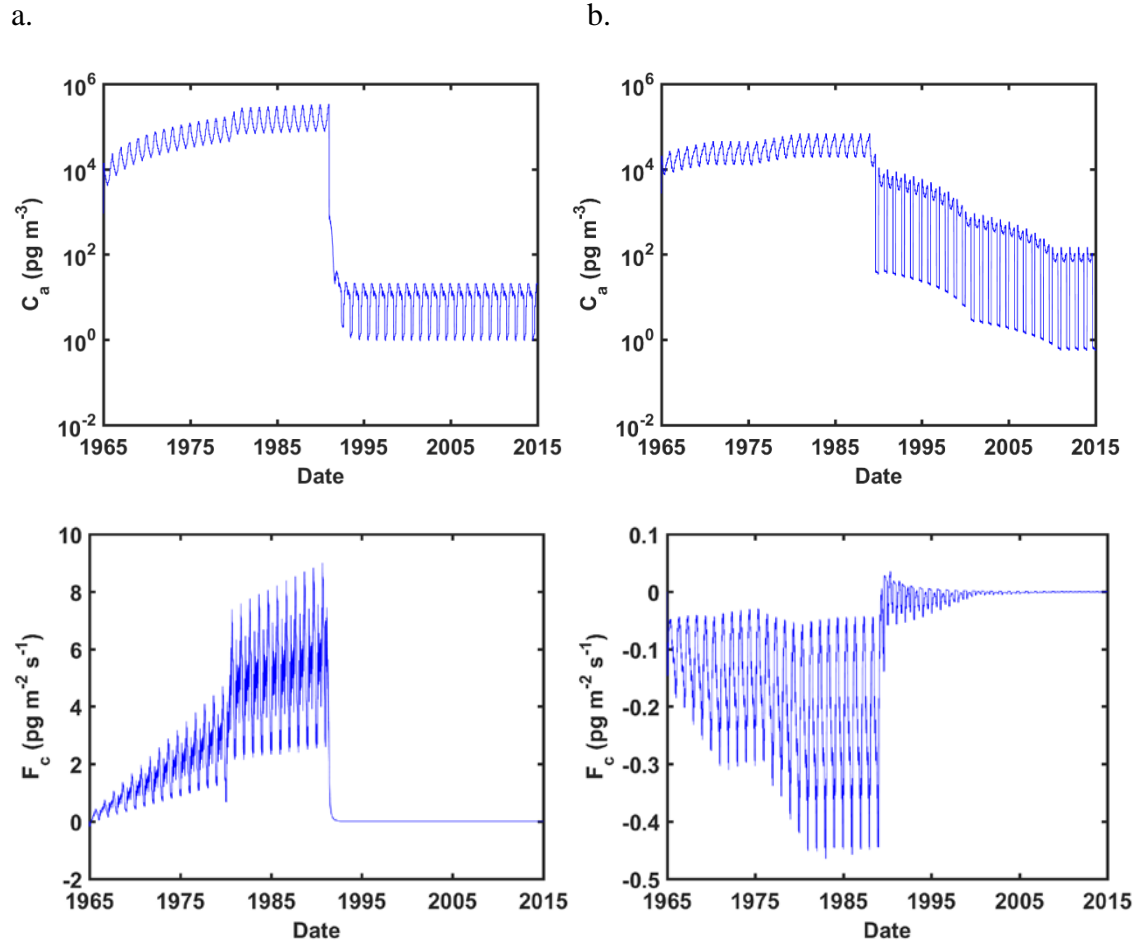
^g rural coastal (Zhang et al., 2008)

^h agricultural soils (Kumari et al., 1996)

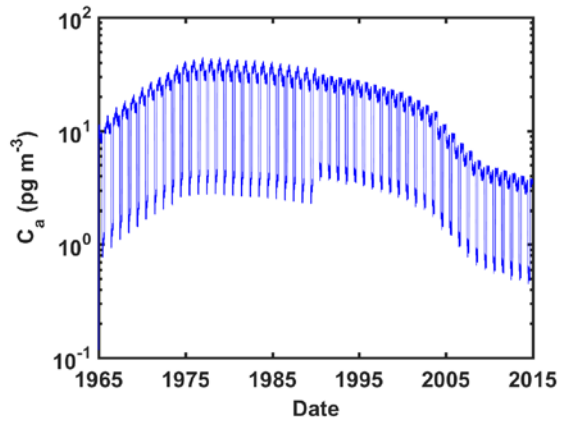
ⁱ agricultural or urban soils (Sharma et al., 2014)

^j agricultural soils (Ramesh et al., 1991)

Fig. S2. Multidecadal 1D model predicted concentrations, c_a (pg m^{-3}), in the atmospheric boundary layer and diffusive air-surface exchange fluxes, F_c ($\text{pg m}^{-2} \text{s}^{-1}$), of (a) α -HCH, (b) p,p' -DDT, (c) PCB28, (d) PCB153 concentrations in the atmospheric boundary layer, c_a , (upper) and diffusive air-surface exchange fluxes, F_c (positive = upward, negative = downward; lower) in the southernmost zone of India ($7.4\text{-}11.2^\circ\text{N}$) 1965-2014.



c.



d.

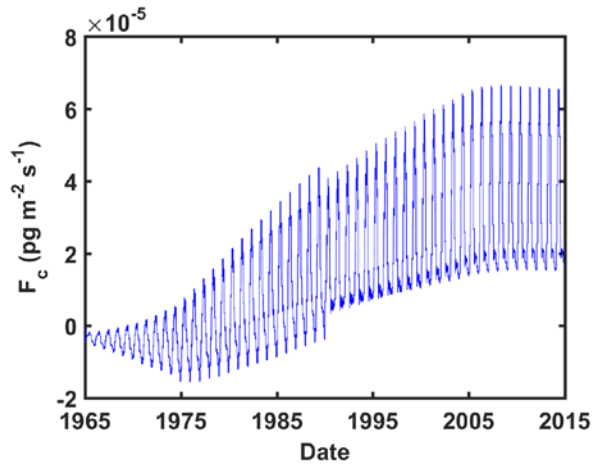
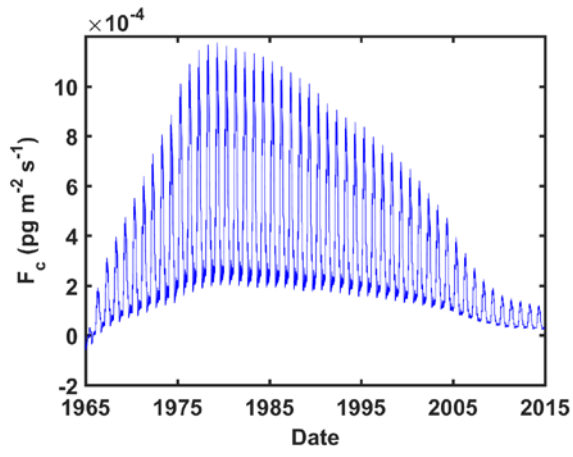
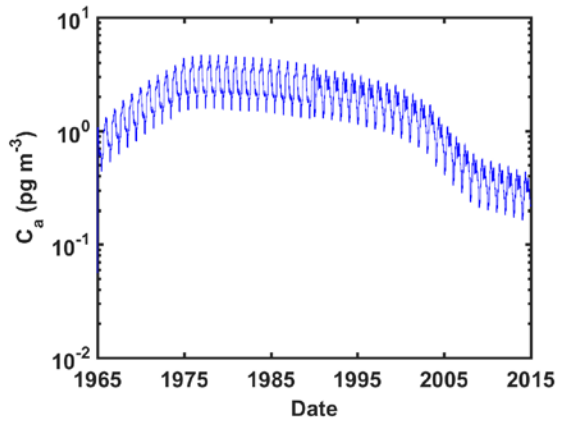
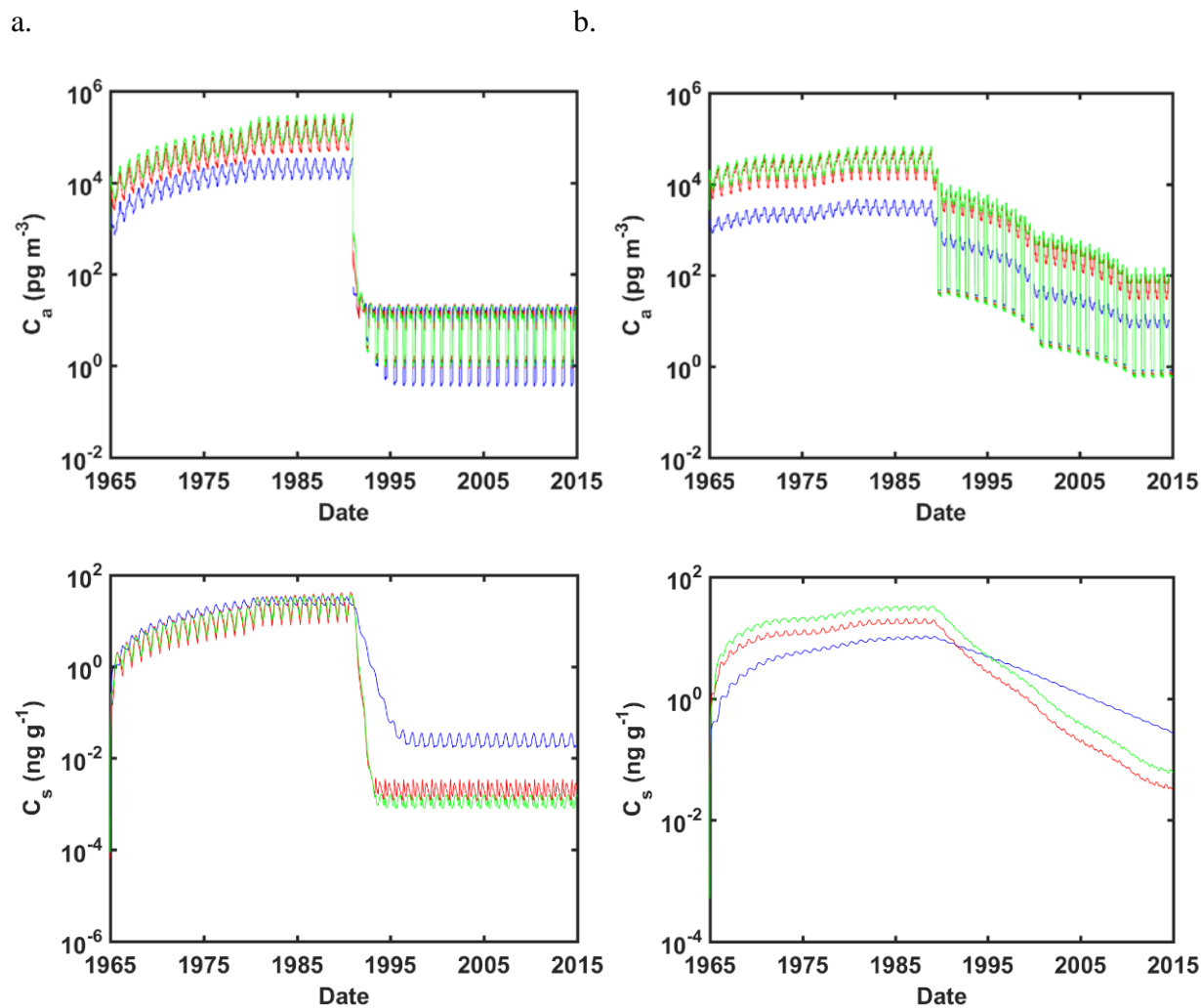
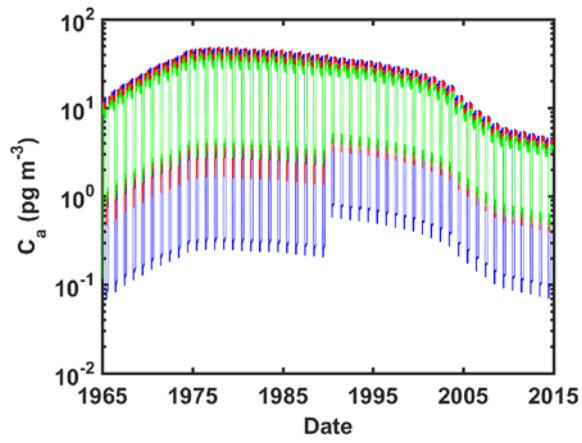


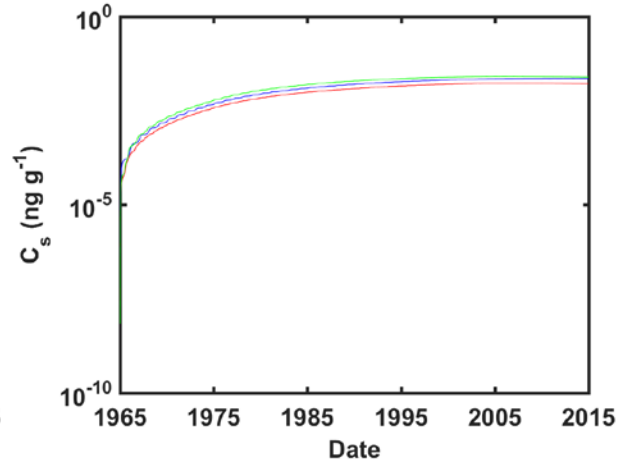
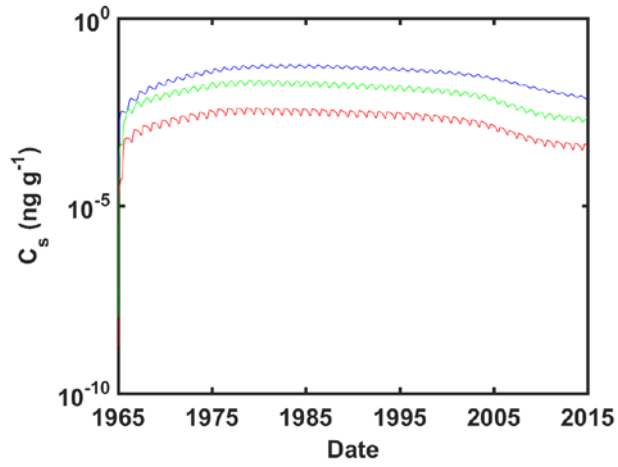
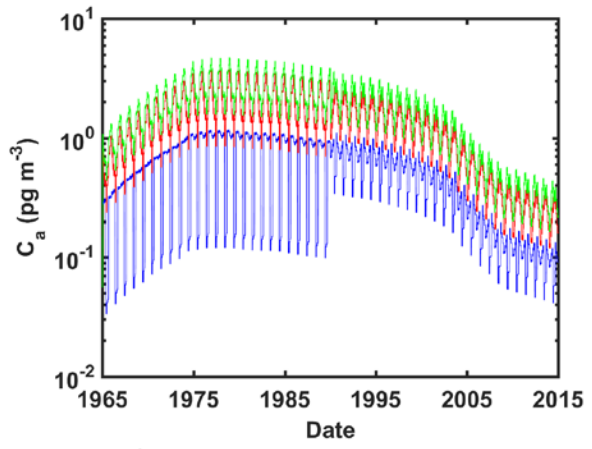
Fig. S3. Multidecadal 1D model predicted concentrations in the atmospheric boundary layer, c_a , (upper), and topsoil (lower) of (a) α -HCH, (b) p,p' -DDT, (c) PCB28, (d) PCB153 in a northern (29.7-33.4°N, blue), central (18.5-22.3°N, red), and southern (7.4-11.2°N, green) zone of India 1965-2014.



c.



d.



S2.2.3 Model sensitivities

Sensitivities of the 1D multi-media mass balance box model output parameters are listed in Table S7. The effect of monsoon on multicompartmental cycling is studied using a fictive no-monsoon scenario, which assumes no air concentration drop at the onset of the monsoon season into the BL box of the northern most zone (but preserves mean of non-monsoon months during the monsoon months), and no seasonal change of the wet deposition flux and the mixing height (but replace the scavenging coefficient W_t , and BL depth, h_{mix} , by the respective mean of non-monsoon months during the monsoon months) (Table S8).

Table S7. Sensitivities of 1D multi-media mass balance box model output parameters to input data variation

Input parameter studied	Variation (lower / upper) against default (S1.4.2)	Sensitivity	
		Low	Linear or high
k_{OH}	$\times 0.33 / \times 3$	c_a of all	with background advection c_a of HCH and PCB28
k_{soil}	$\times 0.33 / \times 3$	c_s and F_c of PCB153	c_s and F_c of HCH, DDT (most), PCB28
$F_{emission}$	$\times 0.33 / \times 3$	c_a of HCH, PCB28	c_a almost linear for DDT, PCB153
h_{mix}	$\times 0.33 / \times 3$	c_a of HCH, PCB28	c_a almost linear for DDT, PCB153
Daily removal from residual layer (vertical dilution)	Set to 0 / $\times 0.33 / \times 3$	c_a of all	
c_a bckgrd	Set to 0	c_a of DDT, PCB153	c_a of HCH, PCB28

Table S8. Comparison of 1D model predicted concentrations in air (pg m^{-3}) and soil (pg g^{-1}) under historic emissions and climate (S1.4.2) vs. under historic emissions but a fictive no-monsoon scenario (see S2.2.3, above) in the southern zone (7.4-11.2°N) 2014. Pre-monsoon = May average, monsoon = June average.

	Air				Soil	
	Pre-monsoon		Monsoon		Monsoon	
	Historic	No-monsoon	Historic	No-monsoon	Historic	No-monsoon
α -HCH	11	11	1.4	13	1.1	1.3
<i>p,p'</i> -DDT	70	70	75	104	59	28
PCB28	3.3	3.3	0.74	3.6	1.18	1.21
PCB153	0.43	0.43	0.38	0.61	23	20

References

- Ackermann, I.J., Hass, H., Memmesheimer, M., Ebel, A., Binkowski, F.S., Shankar, U., 1998. Modal aerosol dynamics model for Europe: Development and first applications. *Atmos. Environ.* 32, 2981–2999.
- Anderson, P.N.; Hites, R.A., 1996. OH radical reactions: The major removal pathway for polychlorinated biphenyls from the atmosphere. *Environ. Sci. Technol.* 30, 1756–1763.
- Bao, Z., Haberer, C.M., Maier, U., Beckingham, B., Amos, R.T., Grathwohl, P., 2016. Modeling short-term concentration fluctuations of semi-volatile pollutants in the soil–plant–atmosphere system. *Sci. Total Environ.* 569–570, 159–167.
- Batjes, N.H, 1996. Total carbon and nitrogen in the soils of the world. *Europ. J. Soil Sci.* 47, 151–163.
- Beyer, A., Mackay, D., Matthies, M., Wania, F., Webster, E., 2000. Assessing long-range transport potential of persistent organic pollutants. *Environ. Sci. Technol.* 34, 699–703.
- Breivik, K., Sweetman, A., Pacyna, J.M., Jones, K.C, 2007. Towards a global historical emission inventory for selected PCB congeners – a mass balance approach. 3. An update. *Sci. Total Environ.* 377, 296–307.
- Brubaker, W., Hites, R.A., 1998. OH reaction kinetics of gas-phase α - and γ -hexachlorocyclohexane and hexachlorobenzene. *Environ. Sci. Technol.* 32, 766–769.
- Bruhn, R., Lakaschus, S., McLachlan, M.S., 2003. Air/sea gas exchange of PCBs in the southern Baltic sea, *Atmos. Environ.* 37, 3445–3454.
- Calamari, D., Bacci, E., Focardi, S., Gaggi, C., Morosini, M., Vighi, M., 1991. Role of plant biomass in the global environmental partitioning of chlorinated hydrocarbons. *Environ. Sci. Technol.* 25, 1489–1495.
- Castro-Jiménez, J., Berrojalbiz, N., Wollgast, J., Dachs, J., 2012. Polycyclic aromatic hydrocarbons (PAHs) in the Mediterranean Sea: Atmospheric occurrence, deposition and decoupling with settling fluxes in the water column, *Environ. Pollut.* 166, 40–47.
- Chen, F., Dudhia, J., 2001. Coupling an advanced land surface–hydrology model with the Penn State-NCAR MM5 modeling system. Part I: Model implementation and sensitivity. *Mon. Weather. Rev.* 129, 569–585.

- Chou, M., Suarez, M., 1994. An efficient thermal infrared radiation parameterization for use in general circulation models, NASA Technical Memorandum No. 104606, Vol. 3, NASA Goddard Space Flight Centre, Greenbelt, USA.
- Degrendele, C., Okonski, K., Melymuk, L., Audy, O., Kohoutek, J., Čupr, P., 2016. Pesticides in the atmosphere: a comparison of gas-particle partitioning and particle size distribution of legacy and current-use pesticides. *Atmos. Chem. Phys.* 16, 1531–1544.
- Devi, S., Yadav, B.P., 2015. Regional characteristics of the 2014 southwest monsoon. In: *Monsoon 2014 – a report* (Pai, D.S., Bhan, S.C., eds.), India Meteorological Department, Pune, pp. 1–17
- Draxler, R.R., Rolph, G.D., 2003. HYSPLIT (HYbrid Single-Particle Lagrangian Integrated Trajectory), NOAA Air Resources Laboratory, Silver Springs, USA. Available from: <http://www.arl.noaa.gov/ready/hysplit4.html>.
- Dunne, K.A., Willmott, C.J., 1996. Global distribution of plant-extractable water capacity of soil. *Int. J. Climatol.* 16, 841–859.
- Emmons, L.K., Walters, S., Hess, P. G., Lamarque, J.F., Pfister, G.G., Fillmore, D., Granier, C., Guenther, A., Kinnison, D., Laepple, T., Orlando, J., Tie, X., Tyndall, G., Wiedinmyer, C., Baughcum, S.L., Kloster, S., 2010. Description and evaluation of the Model for Ozone and Related chemical Tracers, version 4 (MOZART-4), *Geosci. Model Dev.* 3, 43–67.
- EU, 1996. Technical guidance document in support of the commissions directive 5 93/67/EEC on risk assessment for the notified substances and the commission regulation (EC) 1488/94 on risk assessment for existing substances. European Commission, Brussels.
- Fasullo, J., Webster, P.J., 2003. A hydrological definition of Indian monsoon onset and withdrawal. *Journal of Climate* 16, 3200–3211.
- Finizio, A., Mackay, D., Bidleman, T., Harner, T., 1997. Octanol-air partition coefficient as a predictor of partitioning of semi-volatile organic chemicals to aerosols. *Atmos. Environ.* 31, 2289–2296.
- Gasic, B., MacLeod, M., Klánová, J., Scheringer, M., Ilić, P., Lammel, G., Pajović, A., Breivik, K., Holoubek, I., Hungerbühler, K., 2010. Quantification of sources of PCBs to the atmosphere in urban areas: A comparison of cities in North America, Western Europe and former Yugoslavia. *Environ. Pollut.* 158, 3230–3235.
- Grell, G.A., Devenyi, D., 2002. A generalized approach to parameterizing convection combining ensemble and data assimilation techniques. *Geophys. Res. Lett.* 29, 1693.
- Hansen, K.M., Christensen, J.H., Brandt, J., Frohn, L.M., Geels, C., 2004. Modelling atmospheric transport of α -hexachlorocyclohexane in the Northern Hemisphere with a 3-D dynamical model: DEHM-POP. *Atmos. Chem. Phys.* 4, 1125–1137.
- Harner, T., Bidleman, T.F., Jantunen, L.M.M., Mackay, D., 2001. Soil-air exchange model of persistent pesticides in the U.S. Cotton Belt. *Environ. Toxicol. Chem.* 20, 1612–1621.
- Hippelein, M., McLachlan, M. S., 1998. Soil/air partitioning of semivolatile organic compounds. 1. Method development and influence of physical-chemical properties. *Environ. Sci. Technol.* 32, 310–316.
- Hornsby, A.G., Wauchope, R.D., Herner, A., 1996. *Pesticide properties in the environment*. Springer, New York, 227 pp.
- IMD, 2014. Monsoon season (June – September) 2014, *Climate Diagnostic Bulletin of India*, National Climate Centre, Indian Meteorological Department, Pune, India, 23 pp.
- Jaenicke, R., 1988. *Aerosol physics and chemistry*. Landolt-Börnstein Neue Ser. 4b, 391–457.
- Janjic, Z.I., 1994. The Step-Mountain Eta Coordinate Model - Further developments of the convection, viscous sublayer, and turbulence closure schemes. *Mon. Weather. Rev.* 122, 927–945.
- Jury, W.A., Spencer, W.F., Farmer, W.J., 1983. Behaviour assessment model for trace organics in soil: I. Model description. *J. Env. Qual.* 12, 558–564.
- Karickhoff, S.W., 1981. Semi-empirical estimation of sorption of hydrophobic pollutants on natural sediments and soils. *Chemosphere* 10, 833–846.
- Kumari, B., Singh, R., Madan, V.K., Kumar, R., Kathpal, T.S., 1996. DDT and HCH compounds in soils, ponds and drinking water of Haryana, India. *Bull. Environ. Contam. Toxicol.* 57, 787–793.

- Lammel, G., Stemmler, I., 2012. Fractionation and current time trends of PCB congeners: Evolvement of distributions 1950-2010 studied using a global atmosphere-ocean general circulation model. *Atmos. Chem. Phys.* 12, 7199–7213.
- Lammel, G., Klöpffer, W., Semeena, V.S., Schmidt, E., Leip, A., 2007. Multicompartmental fate of persistent substances: Comparison of predictions from multi-media box models and a multicompartment chemistry-atmospheric transport model, *Environ. Sci. Pollut. Res.* 14, 153–165.
- Landlová, L., Čupr, P., Franců, J., Klánová, J., Lammel, G., 2014. Composition and effects of inhalable size fractions of atmospheric aerosols in the polluted atmosphere. Part I. PAHs, PCBs and OCPs and the matrix chemical composition. *Environ. Sci. Pollut. Res.* 21, 6188–6204.
- Li, Y.F., Scholtz, M.T., van Heyst, B.J., 2000. Global gridded emission inventories of α -hexachlorocyclohexane. *J. Geophys. Res.* 102, 6621–6632.
- Li, N., Wania, F., Lei, Y.D., Daly, G.L., 2003. A comprehensive and critical compilation, evaluation, and selection of physical–chemical property data for selected polychlorinated biphenyls. *J. Phys. Chem. Ref. Data* 32, 1545–1590.
- Lin, Y.L., Farley, R.D., Orville, H.D., 1983. Bulk parameterization of the snow field in a cloud model. *J. Clim. Appl. Meteor.* 22, 1065–1092.
- Mackay, D., Shiu, W.Y., Ma, K.C., Lee, S.C., 2006. *Physical-Chemical Properties and Environmental Fate for Organic Chemicals*, Vol. 4, CRC Press, Boca Raton, USA, 970 pp
- McLachlan, M.S., Horstmann, M., 1998. Forests as filters of airborne organic pollutants: A model, *Environ. Sci. Technol.* 32, 413–420.
- Meijer, S.N., Shoeib, M., Jones, K.C., Harner, T., 2003a. Air-soil exchange of organochlorine pesticides in agricultural soils. 2. Laboratory measurements of the soil-air partition coefficient. *Environ. Sci. Technol.* 37, 1300–1305.
- Meijer, S.N., Shoeib, M., Jantunen, L.M.M., Jones, K.C., Harner, T., 2003b. Air-soil exchange of organochlorine pesticides in agricultural soils – 1. Field measurements using a novel in situ sampling device, *Environ. Sci. Technol.* 2003, 37, 1292–1299
- Mlawer, E.J., Taubman, S.J., Brown, P.D., Iacono, M.J., Clough, S.A., 1997. Radiative transfer for inhomogeneous atmospheres: RRTM, a validated correlated-k model for the longwave. *J. Geophys. Res.*, 102, 16663–16682.
- Mu, Q., Shiraiwa, M., Octaviani, M., Ma, N., Ding, A.J., Su, H., Lammel, G., Pöschl, U., Cheng, Y.F., 2018. Temperature effect on phase state and reactivity controls atmospheric multiphase chemistry and transport of PAHs. *Sci. Adv.* 4, aap7314.
- Mulder, M.D., Heil, A., Kukučka, P., Klánová, J., Kuta, J., Prokeš, R., Sprovieri, F., Lammel, G., 2014. Air-sea exchange and gas-particle partitioning of polycyclic aromatic hydrocarbons in the Mediterranean. *Atmos. Chem. Phys.* 14, 8905–8915.
- NVBDCP, 2009. Operational manual for implementation of malaria programme 2009, Government of India, Directorate of National Vector Borne Disease Control Programme, Directorate General of Health Services Ministry of Health and Family Welfare, New Delhi, 275 pp.
- Octaviani, M., Stemmler, I., Lammel, G., Graf, H.F., 2015. Atmospheric transport of persistent organic pollutants to and from the Arctic under present-day and future climate. *Environ. Sci. Technol.* 49, 3593–3602.
- Pacyna, J.M., Sundseth, K., Cousins, I., 2010. Database of physico-chemical properties and historic/future emission estimates for selected chemicals; D11, ArcRisk project, unpublished, Norwegian Institute for Air Research, Kjeller, Norway.
- Paterson S., Mackay D., 1991. Correlation of the equilibrium and kinetics of leaf-air exchange of hydrophobic organic chemicals. *Environ. Sci. Technol.* 25, 866–871.
- Paterson S., Mackay D., McFarlane C., 1991. A model of organic chemical uptake by plants from soil and the atmosphere. *Environ. Sci. Technol.* 28, 2259–2266.
- Patil, M.N., Patil, S.D., Waghmare, R.T., Dharmaraj, T., 2013. Planetary Boundary Layer height over the Indian subcontinent during extreme monsoon years. *J. Atmos. Solar-Terr. Phys.* 92, 94–99.

- Pozo, K., Harner, T., Lee, S.C., Sinha, R.K., Sengupta, B., Loewen, M., Geethalakshmi, V., Kannan, K., Volpi, V., 2011. Assessing seasonal and spatial trends of persistent organic pollutants (POPs) in Indian agricultural regions using PUF disk passive air samplers. *Environ. Pollut.* 159, 646–653.
- Pringle, K.J.; Tost, H.; Message, S.; Steil, B.; Giannadaki, D.; Nenes, A.; Fountoukis, C.; Stier, P.; Vignati, E.; Lelieveld, J., 2010. Description and evaluation of GMX_e: a new aerosol submodel for global simulations (v1). *Geosci. Model Dev.* 3, 391–412.
- Pryor, S., Gallagher, M., Sievering, H., Larsen, S. E., Barthelmie, R.J., Birsan, F., Nemitz, E., Rinne, J., Kulmala, M., Grönholm, T., Taipale, R., Vesala, T., 2008. A review of measurement and modelling results of particle atmosphere-surface exchange. *Tellus B* 60, 42–75.
- Puri, S., Chickos, J.S., Welsh, W.J., 2001. Determination of vaporization enthalpies of polychlorinated biphenyls by correlation gas chromatography. *Anal. Chem.* 73, 1480–1484.
- Puri, S., Chickos, J.S., Welsh, W.J., 2002. Three-dimensional quantitative structure-property relationship (3D-QSPR) models for prediction of thermodynamic properties of polychlorinated biphenyls (PCBs): enthalpies of fusion and their application to estimates of enthalpies of sublimation and aqueous solubilities. *J. Chem. Inf. Comput. Sci.* 43, 55–62.
- Rajendran, R.B., Venugopalan, V.K., Ramesh, R., 1999. Pesticide residues in air from coastal environment, South India. *Chemosphere* 39, 1699–1706.
- Ramesh, A., Tanabe, S., Murase, H., Subramanian, A., Tatsukawa, R., 1991. Distribution and behavior of persistent organochlorine insecticides in paddy soil and sediments in the tropical environment: a case study in South India. *Environ. Pollut.* 74, 293–307.
- Ruijgrok, W., Davidson, C.I., Nicholson, K.W., 1995. Dry deposition of particles – implications and recommendations for mapping deposition over Europe. *Tellus B* 47, 587–601.
- Schell, B., Ackermann, I.J., Hass, H., Binkowski, F.S., Ebel, A., 2001. Modeling the formation of secondary organic aerosol within a comprehensive air quality model system. *J. Geophys. Res.*, 106, 28275–28293.
- Scheringer, M., Wania, F., 2003. Multimedia models of global transport and fate of persistent organic pollutants. In: *Handbook of Environmental Chemistry* (Fiedler, H., ed.), Vol. 30, pp. 237–269.
- Semeena, S., Lammel, G., 2003. Effects of various scenarios upon entry of DDT and γ -HCH into the global environment on their fate as predicted by a multicompartment chemistry transport model. *Fresenius. Environ. Bull.* 12, 925–939.
- Semeena, V.S., Feichter, J., Lammel, G., 2006. Significance of regional climate and substance properties on the fate and atmospheric long-range transport of persistent organic pollutants – examples of DDT and γ -HCH, *Atmos. Chem. Phys.* 6, 1231–1248.
- Shahpoury, P., Lammel, G., Albinet, A., Sofuoğlu, A., Domanoglu, Y., Sofuoğlu, C.S., Wagner, Z., Ždimal, V., 2016. Model evaluation for gas-particle partitioning of polycyclic aromatic hydrocarbons in urban and non-urban sites in Europe – comparison between single- and poly-parameter linear free energy relationships. *Environ. Sci. Technol.* 50, 12312–12319.
- Sharma, B.M., Bharat, G.K., Tayal, S., Nizzetto, L., Čupr, P., Larssen, T., 2014. Environment and human exposure to persistent organic pollutants (POPs) in India: A systematic review of recent and historical data. *Environ. Int.* 66, 48–64.
- Shen, L., Wania, F., 2005. Compilation, evaluation, and selection of physical–chemical property data for organochlorine pesticides. *J. Chem. Eng. Data* 50, 742–768.
- Sheng, J.J., Wang, X.P., Gong, P., Joswiak, D.R., Tian, L.D., Yao, T.D., Jones, K.C., 2013. Monsoon-driven transport of organochlorine pesticides and polychlorinated biphenyls to the Tibetan Plateau: Three year atmospheric monitoring study. *Environ. Sci. Technol.* 47, 3199–3208.
- Spivakovsky, C.M., Logan, J.A., Montzka, S.A., Balkanski, Y.J., Foreman-Fowler, M., Jones, D.B.A., Horowitz, L.W., Fusco, A.C., Brenninkmeijer, C.A.M., Prather, M.J., Wofsy, S.C., McElroy, M.B., 2000. Three-dimensional climatological distribution of tropospheric OH: update and evaluation. *J. Geophys. Res.* 105, 8931–8980.
- Stockwell, W.R., Kirchner, F., Kuhn, M., Seefeld, S., 1997. A new mechanism for regional atmospheric chemistry modeling. *J. Geophys. Res.*, 102, 25847–25879.

- Stohl, A., Hitznerberger, M., Wotawa, G., 1998. Validation of the Lagrangian particle dispersion model FLEXPART against large scale tracer experiments. *Atmos. Environ.* 32, 4245–4264.
- Stohl, A., Forster, C., Frank, A., Seibert, P., Wotawa, G., 2005. Technical Note: The Lagrangian particle dispersion model FLEXPART version 6.2. *Atmos. Chem. Phys.* 5, 2461–2474.
- Strand, A., Hov, Ø., 1996. A model strategy for the simulation of chlorinated hydrocarbon distributions in the global environment. *Water Air Soil Poll.*, 86, 283–316.
- Stull, R.B., 1988. An introduction to boundary layer meteorology, Kluwer, Dordrecht, the Netherlands, 670 pp.
- UNEP, 2016. Report of the effectiveness evaluation on DDT pursuant to the Article 16 of the Stockholm Convention. Report UNEP/POPS/DDT-EG.6/INF/2, United Nations Environment Programme, Geneva, 11 pp.
- Wang, B., Fan, Z., 1999. Choice of South Asian summer monsoon indices. *Bull. Amer. Meteor. Soc.* 80, 629–638.
- Wang, B., Wu, R., Lau, K.M., 2001. Interannual variability of Asian summer monsoon: Contrast between the Indian and western North Pacific-East Asian monsoons. *J. Clim.* 14, 4073–4090.
- Wania, F.; Daly, G.L., 2002. Estimating the contribution of degradation in air and deposition to the deep sea to the global loss of PCBs. *Atmos. Environ.* 36, 5581–5593.
- Wania, F., McLachlan, M.S., 2001. Estimating the influence of forests on the overall fate of semivolatile organic compounds using a multimedia fate model. *Environ. Sci. Technol.* 35, 582–590
- Wild, O., Zhu, X., Prather, M.J., 2000. Fast-j: Accurate simulation of in- and below-cloud photolysis in tropospheric chemical models. *J. Atmos. Chem.* 37, 245–282.
- Xiao, H., Li, N.Q., Wania, F., 2004. Compilation, evaluation and selection of physic-chemical property data for α -, β - and γ -HCH. *J. Chem. Eng. Data* 49:173–185.
- Zhang, G., Chakraborty, P., Li, J., Balasubramanian, T., Kathiresan, K., Takahashi, S., Subramanian, A., Tanabe, S., Jones, K.C., 2008. Passive sampling of organochlorine pesticides, polychlorinated biphenyls, and polybrominated diphenyl ethers in urban, rural and wetland sites along the coastal length of India. *Environ. Sci. Technol.* 42, 8218–8223.
- Zhong, G., Xie, Z., Möller, A., Halsall, C., Caba, A., Sturm, R., Tang, J., Zhang, G., Ebinghaus, R., 2012. Currently used pesticides, hexachlorobenzene and hexachlorocyclohexanes in the air and seawater of the German Bight (North Sea), *Environ. Chem.* 9, 405–414.
- Zhu, Q.Q., Zheng, M.H., Liu, G.N., Zhang, X., Dong, S.J., Gao, L.R., Liang Y., 2017. Particle size distribution and gas–particle partitioning of polychlorinated biphenyls in the atmosphere in Beijing, China. *Environ. Sci. Pollut. Res.* 24, 1389–1396.